

Signature of Sinking Streams on Calcarenite Rock Study Using Geophysical and Geochemical Investigation in Ayankulam Area, South Tamilnadu, India

Antony Ravindran A (✉ antonicogeo@gmail.com)

V.O.Chidambaram College

Antony Alosanai Promilton A

Manonmaniam Sundaranar university

Vinoth Kingston J

V.O.Chidambaram College

Richard Abishek S

V.O.Chidambaram College

Aswin S K

V.O.Chidambaram College

Abinaya R

V.O.Chidambaram College

Research Article

Keywords: Sinking Stream, Karst Formation, Square array, Magneto telluric and Dry fall out

Posted Date: September 21st, 2022

DOI: <https://doi.org/10.21203/rs.3.rs-1784389/v3>

License:  This work is licensed under a Creative Commons Attribution 4.0 International License.

[Read Full License](#)

Abstract

Ayankulam is the trending one recently during the 2021 monsoon of India. Despite a large supply of water from the Nambiar canal for five days, the village's fabled well was unable to fill. When the district collector and IIT team came, they assessed the community and noted that the wells' geological makeup was classified as a karst formation (as per e-news sited in The New Indian Express dated 03/12/2021). There might be some sinking stream that might link this well. Karst topography of calcarenite rocks is the reason for groundwater movement beneath the subsurface for not filling the well. One of the most crucial elements of nature's water supplies is groundwater. Groundwater has to be explored more thoroughly since demand for it rises as the population grows. To determine the existence of usable groundwater for irrigation purposes in the study area Geophysical (Azimuthal square array method and Magnetotelluric method) and Geochemical investigations were done. The Azimuthal Square array method covers 360° coverage of subsurface resulting in fracture orientation of rock to determine the weak/strong zones in different rock types. The Magnetotelluric method scans the subsurface rock and provides information about Geological formation, Weak zone where water oozes out, depth and movement of groundwater. Water samples were collected in and around the "Sinking Stream" origin well and its associated open and tube wells from the study area. The combination of Square Array, MT, Water quality, and quantity study focuses on the Trapped Aquifer system of sinking streams in all water bodies and wells. The movement of groundwater seems to be increasing in Seashore areas such as Uvari and Karikovil are identified relating its water samples from deep bore wells quality and sinking stream water quality. The heavy rainfall and hydrostatic pressure of predominant rock on eroded Calcarenite lime formation create water "Dry fall out" resulting in Sinking streams in the Ayankulam area.

Introduction

Surface geophysical methods have a wide range of applications for studying water resources in arid and semiarid environments. Geophysical methods enable continuous scanning of subsurface soils and water saturation, both of which are critical in remote arid areas. The main objective of the study area is to identify the fracture zone and associated sinking streams of karst topography nature, for which Azimuthal square array resistivity, Magnetotelluric, and Groundwater quality methods are used. It is carried out for suitable soil, rock thickness, and groundwater in the calcareous terrain. Secondary porosity and groundwater salinity control the resistivity of fractured rocks. The use of electrical methods for ground-water explorations and assessments has a number of benefits, including Reduced requirement for borehole drilling and direct groundwater sampling, low-cost data gathering enabling quick monitoring of broad regions, and better placement of monitoring wells Groundwater salinity, which is easily interpreted in terms of groundwater quality, controls electrical conductivity/resistivity.

A stream that loses water as it flows downstream is referred to as a "sinking stream." Because the water table is below the bottom of the stream channel, the water seeps into the ground and replenishes the local groundwater. A gaining stream (or effluent stream), on the other hand, increases in water volume as it draws water from the nearby aquifer further downstream. The sinking streams created a hydraulic

connection with the karst aquifer by pouring into the potentiometric surface through the ponor zone (Koiti, O., et al. 2022). Physical interactions between these two elements combine in sinking streams' groundwater movement; these interactions are particularly important during floods or low water support (Bailly-Comte, V., et al. 2010).

The study area is a part of the coastal area. The study contains, soil, clay-rich soil, calcrete alluvium deposits, sandstone, with Calcarenite or Leptinite, and weathered gneissic rock with basement rock. The study area is located between N 8°18.114', E 77°51.086' of Tirunelveli District, Tamil Nadu is shown in the (Fig. 1). The surface layer is mostly covered by alluvium deposits occurring in all places of the study area. The area enjoys a subtropical climate. The period from May to June is generally hot and dry. The weather is pleasant during the period from December to January. The relative humidity is on average between 79 and 84%. The mean minimum temperature is 22.9°C and the mean maximum daily temperature is 33.5°C respectively. Rainfall data from IMD stations over the period 1901–2000 were utilized and a perusal of the data shows that the normal annual rainfall over the district is 879 mm. Senkottai, Sankarankoil, and the rest of the coast have the highest concentrations, whereas the inland region has a decreasing distribution.

Geological and Hydrogeological Settings

Both porous and fissured strata underlie the district. The district's important aquifer systems are composed of porous sedimentary strata that date from the Tertiary to Recent period and are composed of worn and fractured hard rock formations from the Archaean era. A small area of porous formations made up of Tertiary to Quaternary sandstones, limestones, laterites, and clays may be found in the southeast of the region. Fossiliferous limestone and calcareous sandstone are found sporadically in a coastal area on the southeast side. Southwest of Kudankulam is where the 3 square kilometres of fossiliferous limestone may be discovered. Laterites are exposed in areas across the Radhapuram-Edakkadu, Vijayanarayanam-Kumarapuram, Ittamoli, Nanguneri, and Uramozi regions. Beach sand may be found as a patch along the shore in the Idindakarai-Ovari Belt that is between 50 and 250 metres wide. The river alluvium is found along with the river courses and the thickness of alluvium is restricted to 5-6m. The exploration of the sedimentary tract has revealed that the depth to the basement occurs at a depth of 120mbgl and granular zones are encountered between the depths of 20 to 92mbgl. The yield of bore wells varies from 1-4.5lps.

The aquifer at the shallow depth is under unconfined conditions and the aquifer a depth is under semi-confined to confined conditions. The shallow aquifer is developed through dug wells and the deeper aquifer through tube wells. The dug well can sustain a pumping of 4 to 6 hours while the tube wells can sustain a pumping of 6–8 hours. The degree to which secondary intergranular porosity has developed in crystalline formations without primary porosity determines how well they can hold water. Due to variations in lithology, texture, and structural characteristics, even over very short distances, these aquifers are highly diverse. In the worn mantle and semi-confined circumstances in the fissured and fractured zones at deeper depths, groundwater often occurs under phreatic conditions. The district's weathered zone has a thickness that can reach 30mbgl. Because of the presence of Ca and Mg-bearing

minerals, silicate rocks and basic granulites also played a significant role in the development of black (cotton) soil. At places, composite gneisses were intruded by lit-par-lit Injection of grey granites and grey pegmatites, and bands of charnockite and basic granulites were retrograded into regressive gneisses. The overall multi-kind network lithology status of the rock assigns the name composite gneisses.

Materials And Methods

In the current investigation, geophysical and geochemical techniques are used in order to investigate the sinking stream groundwater occurrence, fractured zone, subsurface lithology, and groundwater flow channel. In the area that was being explored, researchers used the Azimuthal square array approach, the Magnetotelluric method, and the Hydrogeochemistry method.

Azimuthal Square array method:

Geophysical techniques are excellent for mapping underlying rock formations, structures, and lithologies for groundwater concerns. For the detection of water-bearing formations, estimation of their thickness and depth of the water table, and future industrial development, a modified resistivity research known as Azimuthal square array (dc) resistivity is used alongside the geophysical technique. The azimuthal square array method determines electrical anisotropy. A rotating electrode array's apparent resistivity is measured in various directions.

The square-array direct current resistivity sounding method is shown in (Fig 2) and includes inserting four electrodes into the ground to form a square arrangement. Three measurements were taken for each square by Lane, Haeni, and Watson (1995): two perpendicular measurements (α and β) to determine apparent resistivity (ρ_a), and one diagonal measurement (γ) to double-check the measurements (i.e., in a homogeneous isotropic material, $\rho_a \gamma = 0$ and in a homogeneous anisotropic material, $\rho_a \gamma = \rho_{a\alpha} - \rho_{a\beta}$). The equation that is utilised in the process of calculating apparent resistivity is as follows: (Habberjam and Watkins 1967),

$$\rho_a = K(\Delta V/I)$$

where $K = 2\pi a / (2 - \sqrt{2})$ and "a" is the length of the side of a square array.

The square's centre point is used to identify the measurement's location. In order to measure azimuthal apparent resistivity, the square array is rotated around its centre (Habberjam and Watkins 1967). This means that the square array is expanded by a factor of $a\sqrt{2}$ at each azimuth, i.e., the spacing of the electrodes is increased, "a" is the square around a central point expands, currents can be transported to a greater depth, allowing resistivity data to be interpreted as an indicator of the depth (Habberjam and Watkins 1967). The side length of a square array in a homogeneous, isotropic material is almost equal to the penetration depth.

For data collecting, the CRM-500 Aquameter was utilized, which comprises of a resistivity metre, steel electrodes, and a 12 Volts D.C. battery. Each cable set consists of four electrode cables.

MAGNETOTELLURIC METHOD

The magnetotelluric method is helpful for subterranean or deep aquifer investigations. From a geomorphological point of view, landscape tectonic movement, aquifer thickness, freshwater migration, saline intrusion, folded and faulted tectonic movement, and the change of river and coastal silt into meta-sedimentary rock were all studied. There are a number of studies that employ the magnetotelluric approach to locate freshwater discharge, formation, and subsurface geology (Li and Jie (2017), Vozoff Keeva (1991), Abdelzaher et al. (2012), Falgàs (2009), Demirci and Smail (2017)). For the magnetotelluric technique, the ADMT-300S equipment is utilised, along with M, N copper probes that were continually relocated by equal distance and depth of coverage, which was also set to cover 300 m deep. Variation in resistivity democratises the many types of soil, rocks, and shoreline boundaries. Magnetotelluric images were employed to detect the boundary between fresh and salt water. The two electrodes M and N act on the signal generator and receiver at a distance of equal lateral spacing. The data that was received is analysed in Surfer software, which creates 2D and 3D models of subterranean rock intrusions.

HYDROGEOCHEMISTRY

In terms of both time and space, hydro-geochemical processes in groundwater are ever-changing. The geochemical quality of groundwater is influenced by the host rock's features as well as the sorts of underlying rocks. The geochemical composition of groundwater is an integral aspect of scientific groundwater resource management. Groundwater is currently being studied to see if it may be used for drinking, household and industrial needs as well as for irrigation (Aris, (2007); Nagaraju (2016); Krishna Kumar (2014); Khan (2018); Mostafa (2017); Khan & Jhariya (2017); Mostafa (2017); Mostafa (2016); Nagaraju (2007); Nagaraju (2016); Krishna Kumar (2014); Khan & Jhariya (2018); Mostafa (2017)). The quality of groundwater is just as important as its quantity. Every groundwater contains dissolved materials in the solution that are collected from the place because of the flow of the water. To meet the objectives, groundwater samples from diverse locations are collected and analysed to evaluate their quality. Because samples are taken at the well's excellent mouth, the water they contain is a composite of groundwater from a variety of aquifer levels. The pH and temperature of the samples were immediately measured in the field. In any water quality inquiry, water samples must be collected and tested. To assess the quality of groundwater, one-liter polythene bottles should be rinsed with the water to be sampled and then filled with groundwater. The obtained sample should be tightly sealed. In order to get a representative sample, the well must be pumped for at least a few minutes. Otherwise, contaminated or stagnant water may be collected.

Color, turbidity, TDS, electrical conductivity, pH, salinity, alkalinity, major cation, and anion analyses are studied. Piper Trilinear Diagram, Box and Whisker Plot, and Wilcox diagram were created using the collected data. In the Piper Plot, the concentration of the major cations and anions is shown as a percentage (percent) concentration. To determine the appropriateness of irrigation water, Wilcox plots Na percent against EC. When determining the salinity level of irrigation water, the EC (electrical conductivity)

test is commonly utilised. Water's sodium percentage (Na%) can also be an essential indicator of whether or not it's suitable for irrigation.

Results And Discussion

AZIMUTHAL SQUARE ARRAY

For tackling groundwater issues, geophysical techniques are the most effective tools for indirect mapping of underlying rock formations, both in terms of their structures and their lithology (Ramanujam, N., et.al 2006, Antony Ravindran, A. 2012). Resistivity studies using azimuthal square arrays (dc) can be used in conjunction with the geophysical approach to detect groundwater bearing formations, as well as to determine how deep, thick, and wide the water table is. This information can be utilised to prepare for future industrial development. The Azimuthal Square Array Method is utilised to ascertain the degree to which the electrical anisotropy can be oriented in different directions. In order to determine the apparent resistivity in a number of different directions, an electrode array is rotated about its central point. Because the majority of mineral-forming soils and rocks have a very high resistivity when they are dry, the resistivity of soils and rocks is typically a function of the quantity and quality of water that is contained inside the pore spaces and fractures of the material. In total, eight resistivity profiles were collected in the NE-SW direction.

Depth sounding curve is plotted between apparent resistivity and 'A' spacing. A plot of the 'A' spacing against the apparent resistivity values acquired from the square array's resistivity zones. The maximum resistivity in this area is 13346-ohm m. At the depth range of 12 to 18m in all profiles, groundwater occurred in the range of resistivity of 120 Ohm.m. The high resistivity of 13346 Ohm.m indicates the Charnockite rock of the study area. The 2D plotting gives details of the apparent resistivity changes in the study area.

Profile 1 covers a subsurface distance of up to 40 meters. At a depth of 8–10 meters, a saturated water zone with resistivity values of 100–120 Ohm.m is discovered. The depth of penetration in profile 2 was fixed at 30 meters. At a depth of 12–14 meters, the freshwater zone was discovered, with resistivity values ranging from 100 to 120 Ohm.m. Profile 3 goes down to a depth of 38 meters. Freshwater with a resistivity of 100–120 Ohm.m was detected at a depth of about 13-16m. Profile 4 data was gathered to a depth of 30 meters, and the freshwater zone was found at a depth of 13–14 meters, with resistivity values ranging from 100 to 120 Ohm.m. Result of the depth vs apparent resistivity for profile 1 to 4 displayed in Fig. 3. The depth of penetration in profile 5 was up to 28 meters. At a depth of 13–15 meters, a saturated freshwater zone was discovered with resistivity values ranging from 100 to 120 Ohm.m. Profile 6 extends about 25 meters below the surface, with a freshwater zone at a depth of 17–19 meters with apparent resistivity of 100–120 Ohm.m. The depth of penetration in profile 7 is up to 28 meters. At a depth of 14–15 meters, the freshwater zone was discovered, with resistivity values ranging from 100 to 120 Ohm.m. Profile 8 has a total depth of 28 meters. At a depth of 14–16 meters, a freshwater zone was discovered with a resistivity of 100–120 Ohm.m. Result of the depth vs apparent resistivity for profile 5 to

8 is shown in Fig. 4. From the top red soil to the bottom charnockite base rock, the overall lithology was discovered. The red soil depth varies from 1 to 5 meters, weathered gneiss was observed between 5 and 12 meters, freshwater zone in calcarenite or leptinite rock was found between 12 and 22 meters, Gneissic rock/Migmatite rock was discovered between 22 and 34 meters, and base rock charnockite was discovered below 34 meters is shown in Table 1.

Table 1
Lithology result from all Profiles.

Depth from (m)	Depth Up to (m)	Formation of Rock	Water identified (yes or no)
0	5	Red soil mix with sand	No
6	12	Weathered gneissic rock	No
13	22	Calcarenite/Leptinite	yes
23	34	Gneissic rock / some Migmatite rock	No
35	54	Charnockite/pegmatite vein intrusion	Below level

Magneto Telluric method

ADMT-300S Water detector is belonging to the category of electrical prospecting's M/T method prospecting. Thoroughly solving problems of different and changeable source intensity of the natural electric field. Now the detector is easy and convenient, with stable source measuring now, high intelligence, and direct viewing of a diagram. Obtaining remarkable achievements in a few decades of field explorations.

Profile 1

Profile 1 covers the area of 30 m distance and depth of 100m across the proposed area. The 2D MT resistivity is a range of 0.22–0.30 Ω .m indicating weathered rock. The water-bearing or flow is indicated in the range from 0.02–0.10 Ω .m at the depth of 30m in the study area.

Profile 2

Profile 2 covers the area of 30 m distance and depth of 100m across the proposed area. The 2D MT resistivity in the range of 0.11–0.14 Ω .m indicates weathered/ hornblende biotite gneiss rock. The water-bearing or flow is indicated ranges from 0.048–0.07 Ω .m. depth of 10m in the study area.

Profile 3&4

Profiles 3 and 4 cover the area of 30 m distance and depth of 300m across the proposed area. The 2D MT resistivity in the range of 0.22–0.28 Ω .m indicates weathered/hornblende gneissic rock. The water-

bearing or flow is indicated in the range from 0.10–0.18 Ω .m and the water-bearing zone is the depth of 150m in the study area.

Profile 5

Profile 5 covers the area of 30m distance and depth of 100m across the proposed area. The 2D MT resistivity is a range of 0.050–0.065 Ω .m indicating weathered/ calcareous rock. The high resistivity range of 0.070–0.076 Ω .m indicates gneissic and hard rock formation.

Profile 6

Profile 6 covers the area of 160m distance and depth of 300m across the proposed area. The 2D MT resistivity is a range of 0.077–0.097 Ω .m indicating weathered/ calcareous rock. The water-bearing or flow is indicated ranges from 0.047–0.067 Ω .m and the water-bearing zone is at depth of 150m in the study area. The high resistivity range of 0.117–0.132 Ω .m indicates gneissic and hard rock formation. The graph for all the profiles were shown in Fig. 5.

Geochemistry:

The groundwater quality evaluation of the study area using geochemical modeling can be used to provide safe drinking and agricultural water to the farmer community. The distribution of different chemical constituents at the lake site can be used as a variation in the alluvium, concrete, and gneiss rock. In general hydrochemistry, the pH of groundwater samples varies from 6.8 to 9.7, which is slightly alkaline. EC of groundwater collected from the study area ranges from 255 to 1070 μ S/cm. The variation of TDS in the sample is between 170 to 705. A few groundwater samples along the calcrete sample have a high concentration of Cl. Groundwater is used for drinking, domestic, irrigational, and industrial purposes in this area. Hence, it is essential to determine its suitability to use for drinking and irrigational purposes. The analytical results were compared with the WHO (1984) The cation exchange process and silicate weathering control the groundwater chemistry in this area. Hydrochemical reaction modeling indicates the release of Ca and adsorption of Mg and Na by ion exchange processes along the groundwater flow path. Other important processes include the dissolution and precipitation of minerals. The groundwater of this area is suitable for domestic purposes except for a few locations where high EC, pH, and other dissolved ions make it unsafe for drinking. The statistical summary of all groundwater samples was displayed in Table 2.

Table 2
Statistical summary of groundwater samples

Parameter	Unit	Min	Max	Average	St. Dev.
pH		6.8	9.7	7.1	7.3
EC	uS/cm	255.0	1070.0	743.0	335.0
TDS	mg/l	170.0	705.0	479.3	209.1
Ca	mg/l	11.0	79.0	58.8	26.5
Mg	mg/l	4.0	23.0	16.9	7.4
Na	mg/l	18.0	94.0	60.6	31.6
K	mg/l	2.0	10.0	6.4	3.4
Fe	mg/l	0.0	0.2	0.0	0.1
Cl	mg/l	31.0	341.0	120.9	89.8
HCO ₃	mg/l	46.0	295.0	222.7	100.5
SO ₄	mg/l	7.0	67.0	37.7	24.9

The Piper diagram is a useful tool for determining geochemical changes in groundwater (Piper, 1944) is shown in Fig. 6. The cation triangle of the Piper plot shows that the no dominant type for the majority of samples (A2, A4, A5, A6, A7, and A8), Ca + dominant consists of two samples seen in the left lower part (A3 and A10) and Na + and K + were found in the right lower part of the cation triangle having two samples (A1 and A9). Anion triangle of the plot shows that the majority of the samples fall on CO₃- and HCO₃- (A2, A3, A4, A5, A6, A7, and A8) type which is seen on the lower left side, and Cl- type consists of three samples (A1, A9, and A10) which are seen on lower right side of Anion triangle. The diamond-shaped part in the Piper plot explains that the majority of samples fall on Na-Ca-HCO₃-Cl type (A2, A3, A5, A7, A8, A9, and A10), sample A1 is of Ca-Mg-HCO₃-Cl type, sample A6 is of Ca-Cl-HCO₃ type and sample A4 is of Ca-Na-Mg-HCO₃ type. The water types of all samples collected are shown in Table 3.

Table 3
Water type of samples collected.

Station ID	Latitude	Longitude	Water type
A1	8.294598	77.84691	Ca ²⁺ -Mg ²⁺ -HCO ₃ -Cl-
A2	8.29018	77.84513	Na ⁺ -Ca ²⁺ -HCO ₃ -Cl-
A3	8.301082	77.83819	Ca ²⁺ -Na ⁺ -Cl-HCO ₃
A4	8.300565	77.84555	Ca ²⁺ -Na ⁺ -Mg ²⁺ - HCO ₃ -Cl-
A5	8.300174	77.85711	Na ⁺ -Ca ²⁺ -Cl-HCO ₃
A6	8.311044	77.84691	Ca ²⁺ -Cl-HCO ₃
A7	8.309605	77.8481	Na ⁺ -Ca ²⁺ -Cl-HCO ₃
A8	8.310438	77.84943	Na ⁺ -Ca ²⁺ -Cl-HCO ₃
A9	8.309809	77.8539	Ca ²⁺ -Na ⁺ -Cl-HCO ₃
A10	8.309453	77.86518	Na ⁺ -Ca ²⁺ -HCO ₃ -Cl-

Wilcox (1955) used the Wilcox diagram to evaluate irrigation waters using percent sodium and specific conductance as shown in Fig. 7. The results of the hydrochemical analysis show that the groundwater samples no. A1, A2, and A9 of the study area are suitable for drinking and domestic purposes. The groundwater is also good for irrigation with low alkalinity and moderates to high salinity hazard from the Wilcox plot.

Conclusion

A quick study of sinking streams on karst topography occurs in the heavy rainfall season. The trapped aquifer system of an open bore and tube wells at the depth of 10m, 20m, 30m, 60m, 100m, 120m, 150m, and 280m of aquifer layers such as Perched, Leaky, Semi-confined, Confined and Unconfined aquifer system for the following depth-wise formations. The present study attempts finding of ooze out water from soft rock/Calcarenite/Leptinite rocks. The rainwater collected on the open well moves at shallow and deeper depths through karst caves or sinking streams and fills the nearby areas wells or water bonds of deep wells.

The resistivity values obtained from the square array resistivity method determine the fractured zone/weathered rock in the study area with an apparent resistivity value of 120-ohm m. The magnetotelluric method clearly provides the information on depth-wise karst caves formed at different depth levels comparing the first profile to the last profile indicating a water flow path with a variation of depth 10m, 20m, 60m for a 5km radius. The groundwater geochemistry relates the concentration of Ca⁺ ions and HCO₃ ions of minimum and maximum values of 11–79 mg/l and 46–295 mg/l with calcareous rock and water interaction resulting in dissolved Ca contents under water on the flow direction path. The

Electrical resistivity method and Magnetotelluric method identify i) Subsurface geology, Cave formations, and Karst rocks and ii) Water gradient and Water flow direction. The origin of the water is identified from groundwater geochemistry. The sinking stream was fall out near trapped leaky aquifer systems which are generated by the cavities of "Lime or Ca" content-rich rocks such as Calcarenite, Leptinite, and Migmatite extending from Ayankulam to the Karikovil area. The underground movement of water from Ayankulam village and finally oozes out near the sea shore area of Karikovil at the depth of around 185m retrieved from the freshwater bore well-constructed in that area is shown in Fig. 8. The groundwater quality also matches with the samples of water collected "Sinking Stream" open well. This will be a useful study for society about how to save this water movement through sinking streams for stopping too much rainwater from getting mixed into the sea. It is referred to as "Submarine Groundwater Discharge," and it describes the process through which subsurface freshwater is mixed with seawater (SGD). A future study is needed on this case for the utilization of the groundwater getting mixed into the sea for public utilities.

Declarations

Acknowledgments

The First author expresses his sincere thanks to Shri. A.P.C.V. Chocka lingam, Secretary and our Principal Dr. C. Veerabhahu, V.O.Chidambaram College, Thoothukudi. The help was extended by Dr. P. Sivasubramanian, Professor and Head, PG and Research Department of Geology, V.O.Chidambaram College, Thoothukudi.

Author Contributions

All authors contributed in conceptualization and design. All authors performed material preparation, data collection and analysis.

Funding – Not available

Data Availability Statement: The datasets generated during and/or analyzed during the current study are available from the corresponding author on reasonable request.

Declarations of Conflicts of Interests

The authors have no conflicts of interest to declare that are relevant to the content of this article.

Ethics Approval Not applicable.

Consent to Participate Not applicable.

Consent for Publication Not applicable

References

1. Habberjam, G. M. (1972). The effects of anisotropy on square array resistivity measurements. *Geophysical prospecting*, 20(2), 249–266. <https://doi.org/10.1111/j.1365-2478.1972.tb00631.x>
2. Habberjam, G. M., & Watkins, G. E. (1967). The use of a square configuration in resistivity prospecting. *Geophysical prospecting*, 15(3), 445–467. <https://doi.org/10.1111/j.1365-2478.1967.tb01798.x>
3. Habberjam, G. M., & Watkins, G. E. (1967). The reduction of lateral effects in resistivity probing. *Geophysical Prospecting*, 15(2), 221–235. <https://doi.org/10.1111/j.1365-2478.1967.tb01785.x>
4. Ravindran, A. A. (2012). Azimuthal square array method and groundwater potential zone in hard rock area in Thoothukudi District, Tamilnadu. *Archives of Applied Science Research*, 4(2), 971–979.
5. Vozoff, K. (1991). The magnetotelluric method. <https://doi.org/10.1190/1.9781560802686.ch8>
6. Khan, R., & Jhariya, D. C. (2018). Hydrogeochemistry and groundwater quality assessment for drinking and irrigation purpose of Raipur City, Chhattisgarh. *Journal of the Geological Society of India*, 91(4), 475–482.
7. Albouy, Y., Andrieux, P., Rakotondrasoa, G., Ritz, M., Descloitres, M., Join, J. L., & Rasolomanana, E. (2001). Mapping coastal aquifers by joint inversion of DC and TEM soundings-three case histories. *Groundwater*, 39(1), 87–97. <https://doi.org/10.1111/j.1745-6584.2001.tb00354.x>.
8. Aris, A. Z., Abdullah, M. H., & Kim, K. W. (2007). Hydrogeochemistry of groundwater in Manukan island, Sabah. *Malaysian Journal of Analytical Sciences*, 11(2), 407–413.
9. Bailly-Comte, V., Martin, J. B., Jourde, H., Sreaton, E. J., Pistre, S., & Langston, A. (2010). Water exchange and pressure transfer between conduits and matrix and their influence on hydrodynamics of two karst aquifers with sinking streams. *Journal of Hydrology*, 386(1–4), 55–66. <https://doi.org/10.1016/j.jhydrol.2010.03.005>
10. Demirci İ, Candansayar ME, Vafidis A, Soupios P (2017) Twodimensional joint inversion of direct current resistivity, radio-magnetotelluric and seismic refraction data: an application fromBafra Plain, Turkey. *J Appl Geophys* 139:316–330. <https://doi.org/10.1016/j.jappgeo.2017.03.002>.
11. Falgàs E, Ledo J, Marcuello A, Queralt P (2009) Monitoringfreshwater– seawater inter face dynamics with audiomagnetotelluric data. *Near Surface Geophysics*. <https://doi.org/10.3997/1873-0604.200903>.
12. Koit, O., Mayaud, C., Kogovšek, B., Vainu, M., Terasmaa, J., & Marandi, A. (2022). Surface water and groundwater hydraulics of lowland karst aquifers of Estonia. *Journal of Hydrology*, 610, 127908. <https://doi.org/10.13140/RG.2.2.13634.86726>
13. Krishna Kumar, S., Bharani, R., Magesh, N. S., Godson, P. S., & Chandrasekar, N. (2014). Hydrogeochemistry and groundwater quality appraisal of part of south Chennai coastal aquifers, Tamil Nadu, India using WQI and fuzzy logic method. *Applied Water Science*, 4(4), 341–350.
14. Lane Jr, J. W., Haeni, F. P., & Watson, W. M. (1995). Use of a square-array direct-current resistivity method to detect fractures in crystalline bedrock in New Hampshire. *Groundwater*, 33(3), 476–485. <https://doi.org/10.1111/j.1745-6584.1995.tb00304.x>

15. Li, J., Pang, Z., Kong, Y., Lin, F., Wang, Y., Wang, G., & Lv, L. (2017). An integrated magnetotelluric and gamma exploration of groundwater in fractured granite for small-scale freshwater supply: a case study from the Boshan region, Shandong Province, China. *Environmental Earth Sciences*, 76(4), 1–12. <https://doi.org/10.1007/s12665-017-6486-z>.
16. Mostafa, M. G., Uddin, S. M., & Haque, A. B. M. H. (2017). Assessment of hydro-geochemistry and groundwater quality of Rajshahi City in Bangladesh. *Applied Water Science*, 7(8), 4663–4671.
17. Nagaraju, A., Muralidhar, P., & Sreedhar, Y. (2016). Hydrogeochemistry and groundwater quality assessment of Rapur area, Andhra Pradesh, South India. *Journal of Geoscience and Environment Protection*, 4(4), 88–99.
18. Obiadi, I. I., Onwuemesi, A. G., Anike, O. L., Ajaegwu, N. E., Anakwuba, E. K., Nwosu, C. M., ... Onuba, O. L. (2013). Determining subsurface fracture characteristics from the azimuthal square array resistivity survey at Igarra, Nigeria. *Pure and Applied Geophysics*, 170(5), 907–916. <https://doi.org/10.1007/s00024-011-0443-7>
19. Ramanujam, N., Murugan, K. N., & Ravindran, A. A. (2006). Azimuthal square array resistivity studies to infer active fault zones in the areas of known seismicity, Kottayam district, Kerala: A case study. *Journal of Indian Geophysical Union*, 10(3), 197–208.

Figures

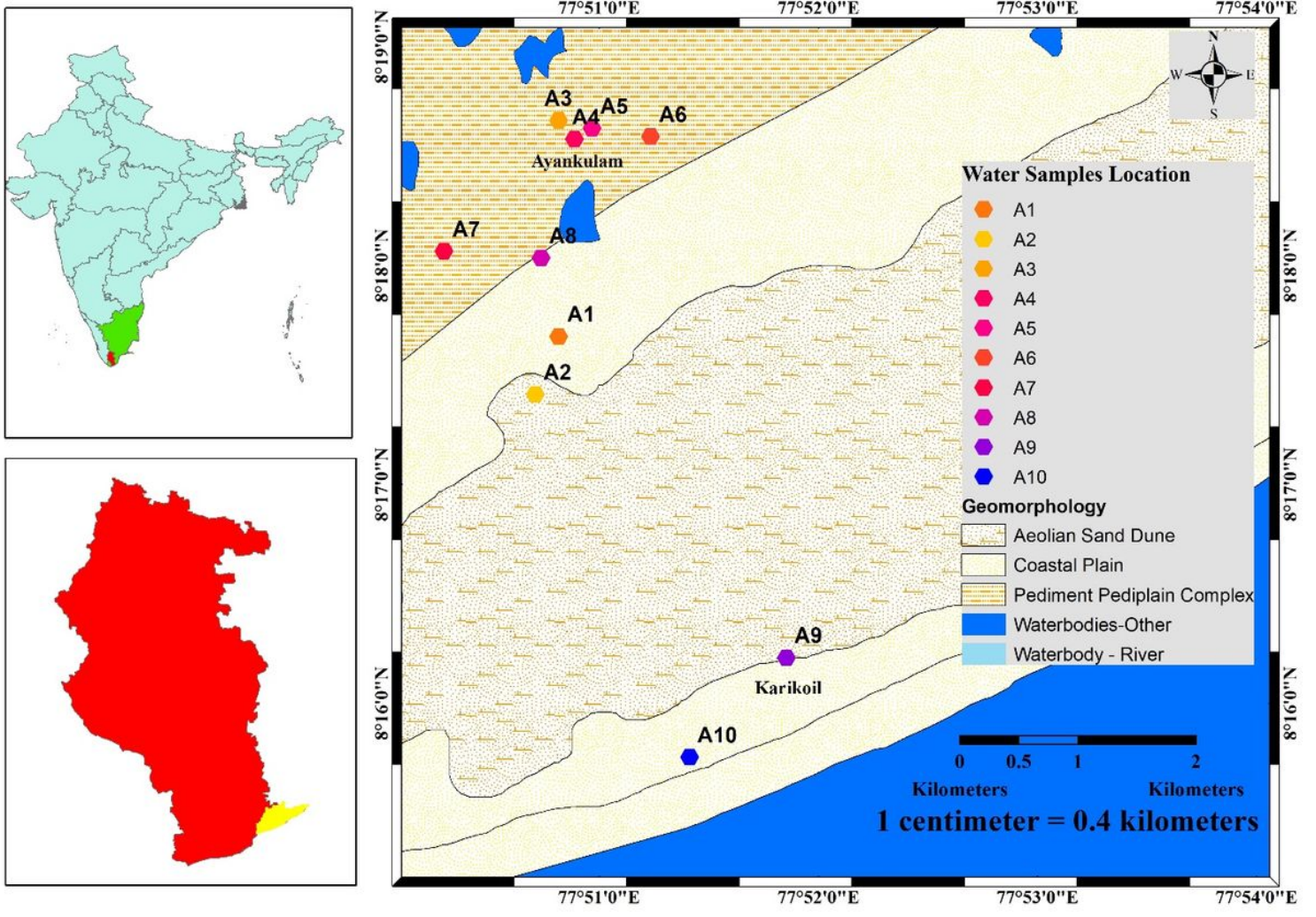


Figure 1

Study Area map.

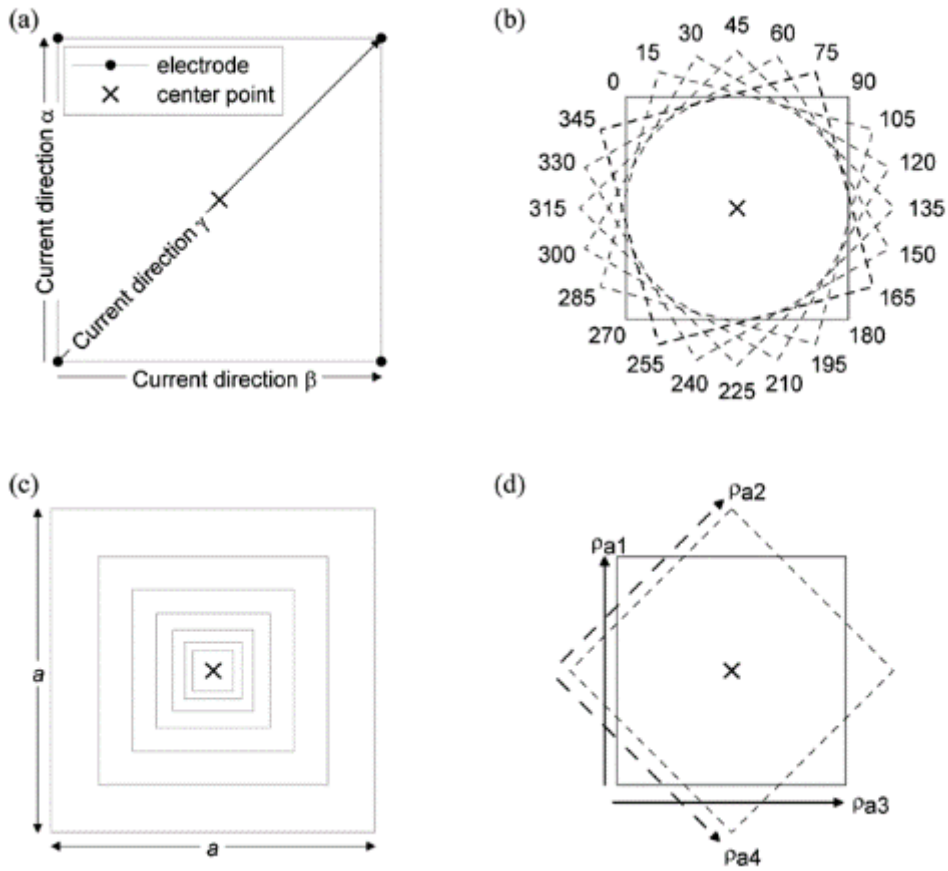


Figure 2

Electrode configuration for Data collection.

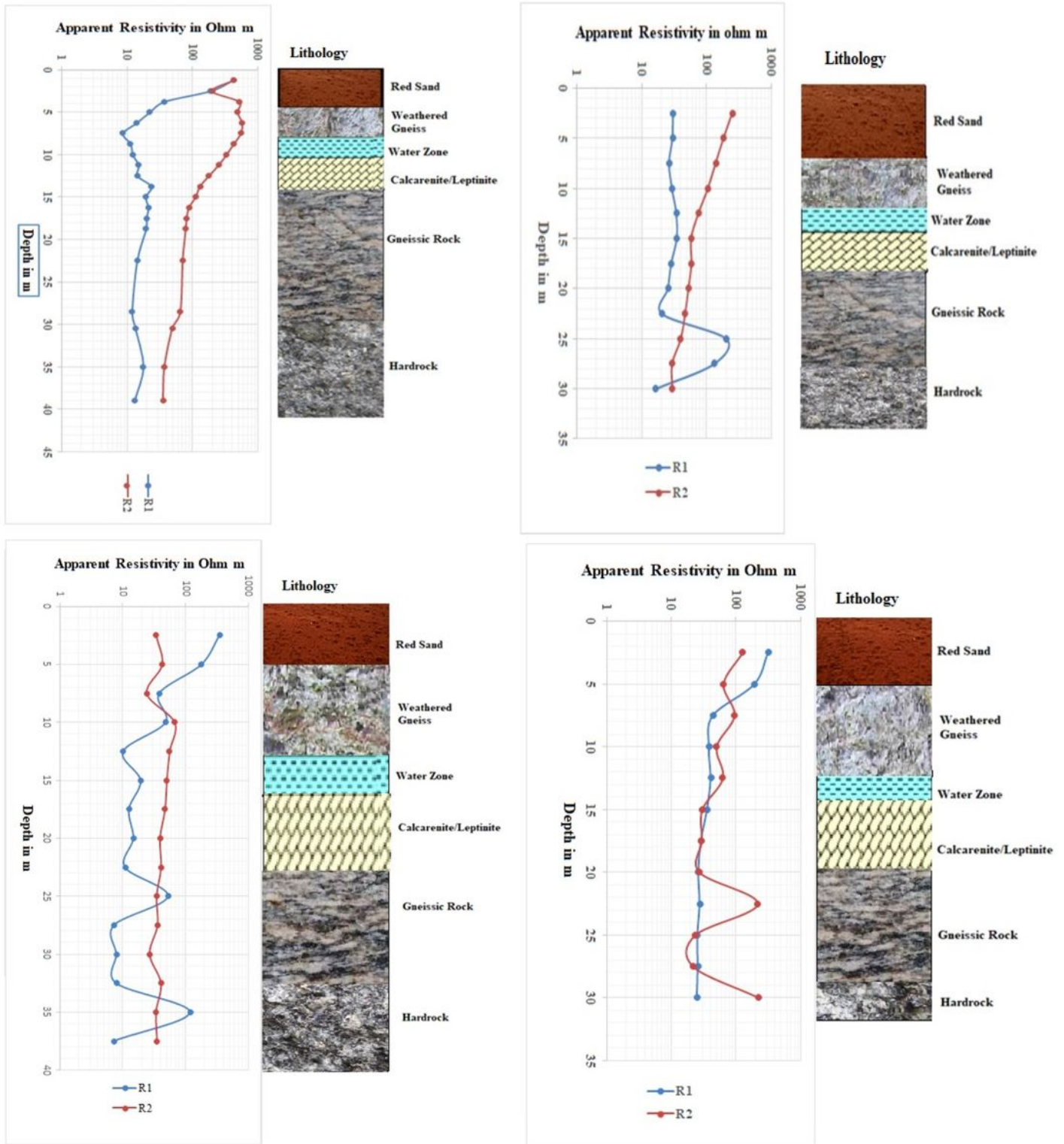


Figure 3

Electrical Resistivity Profile 1 to 4.

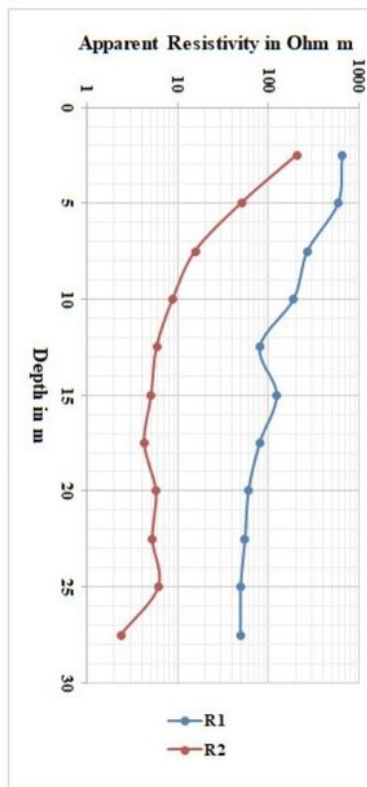
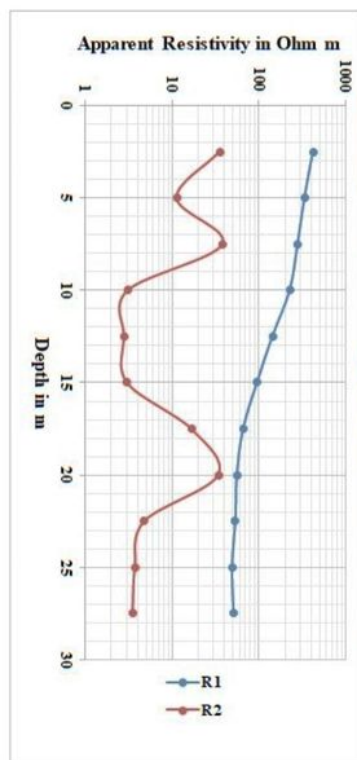
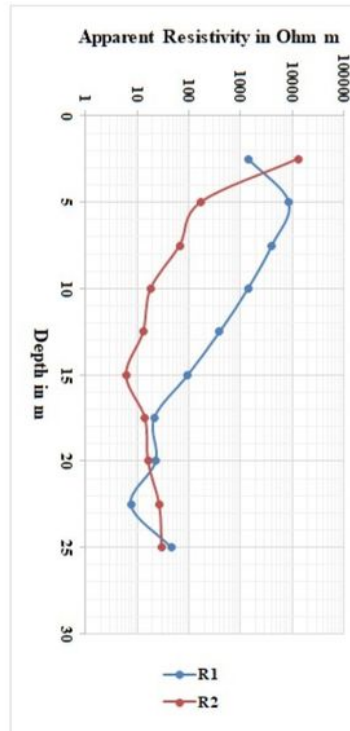
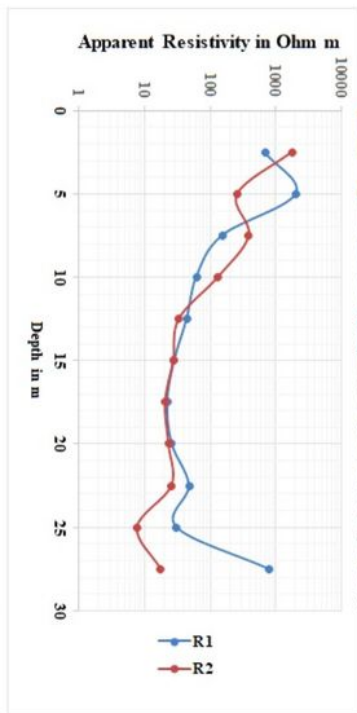


Figure 4

Electrical Resistivity Profile 5 to 8.

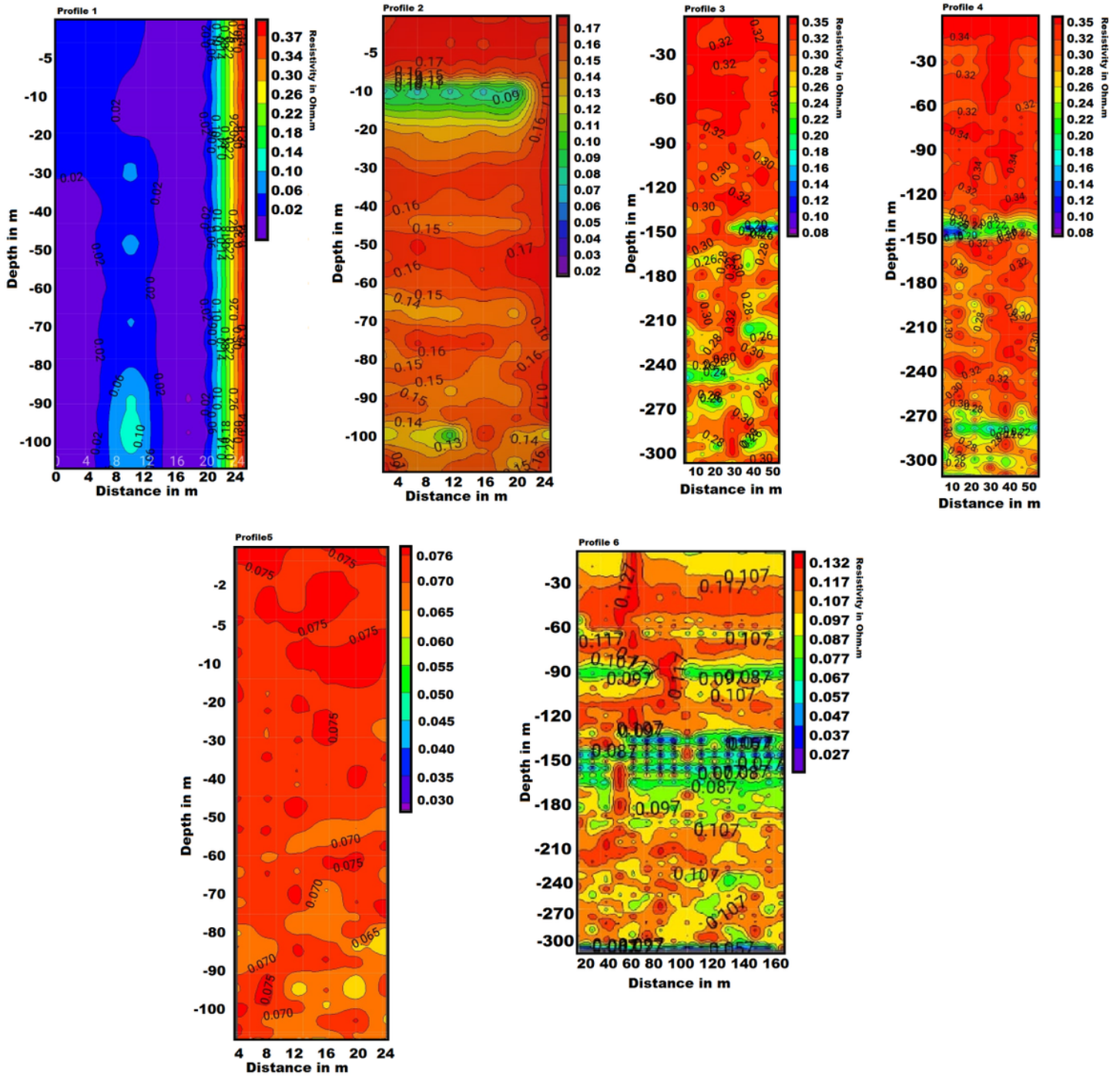


Figure 5

Magnetotelluric Profiles 1 to 6.

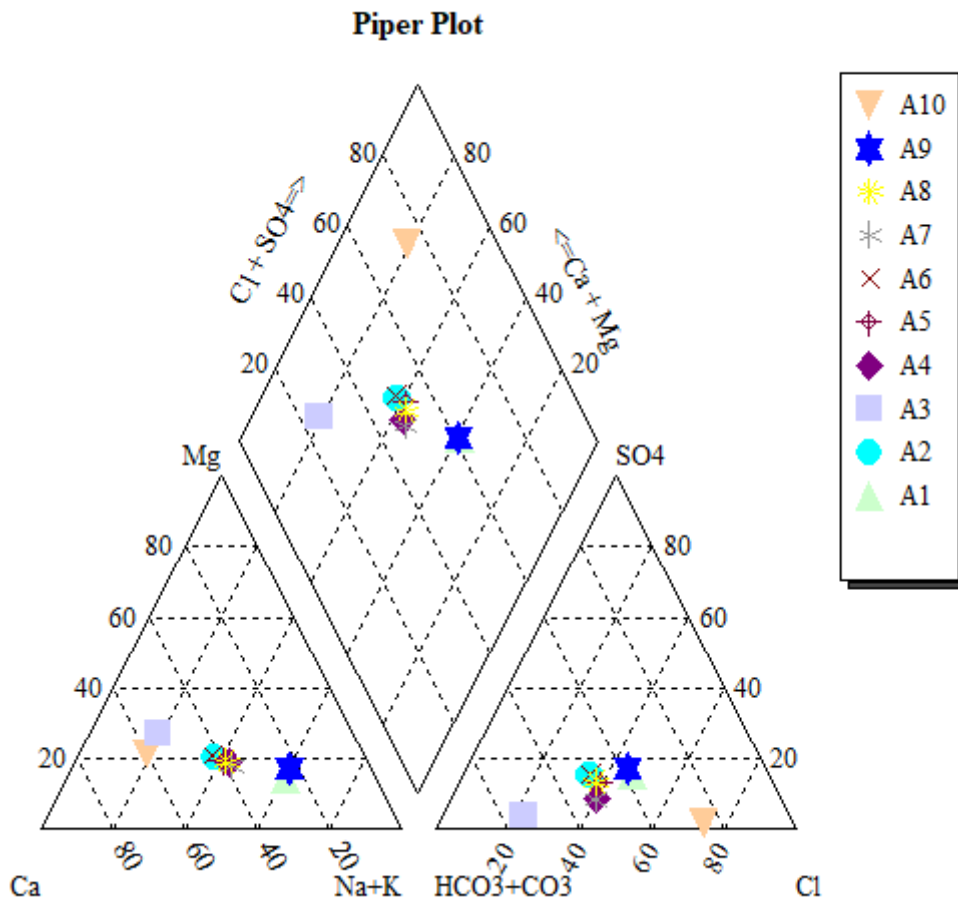


Figure 6

Piper plot for water samples.

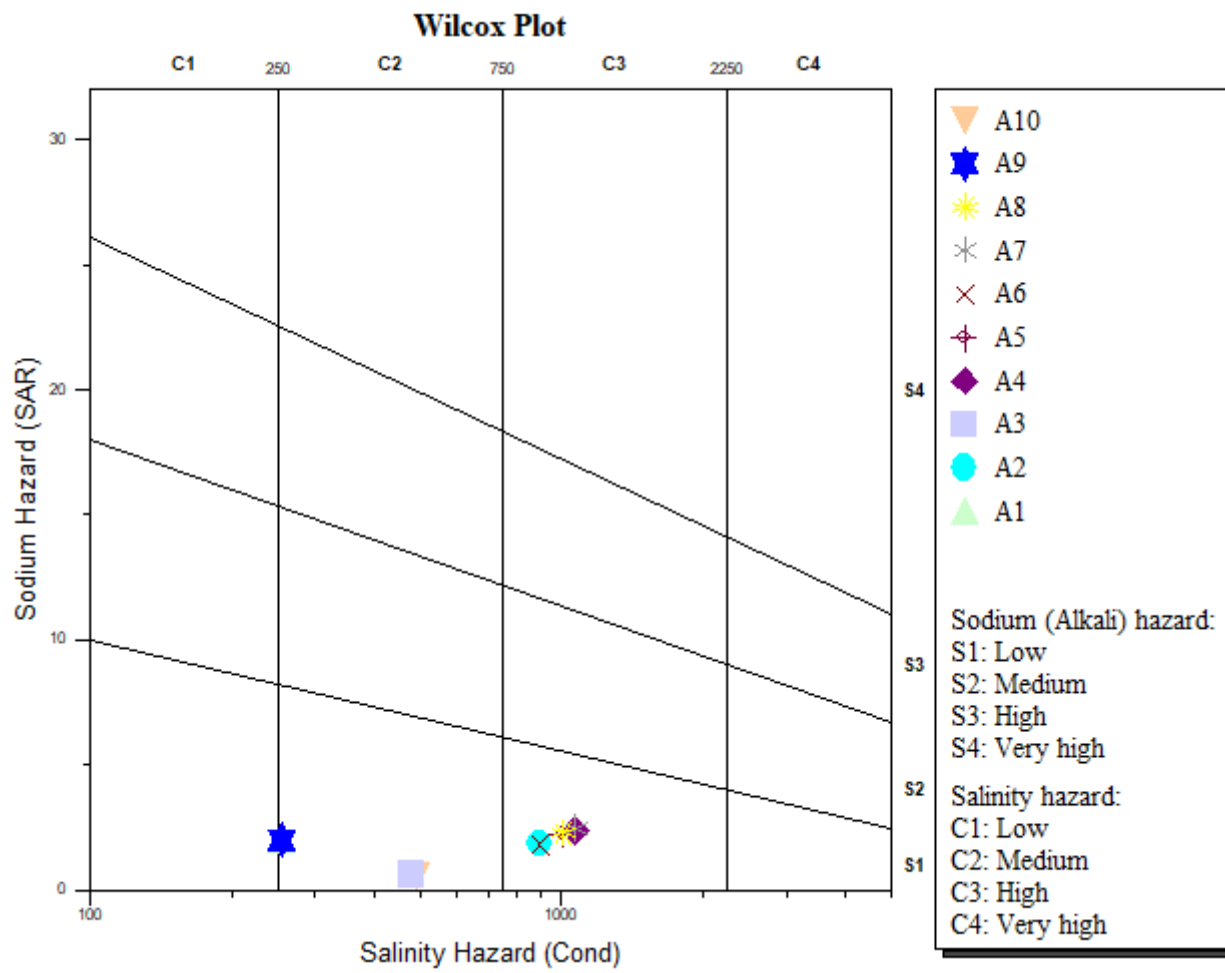


Figure 7

Wilcox plot for water samples.

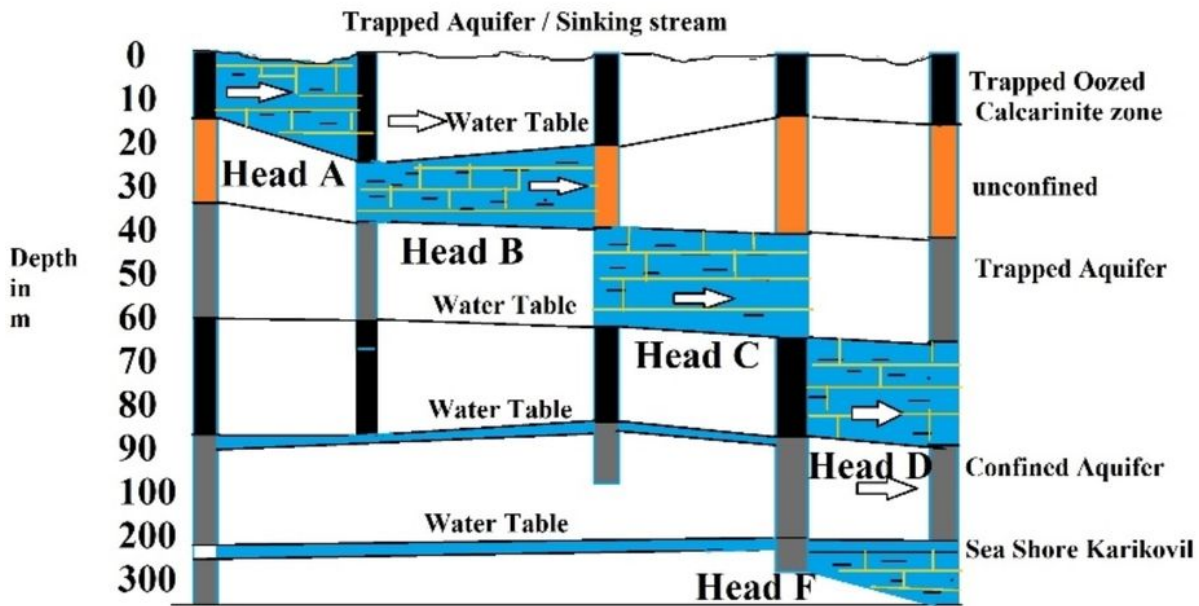
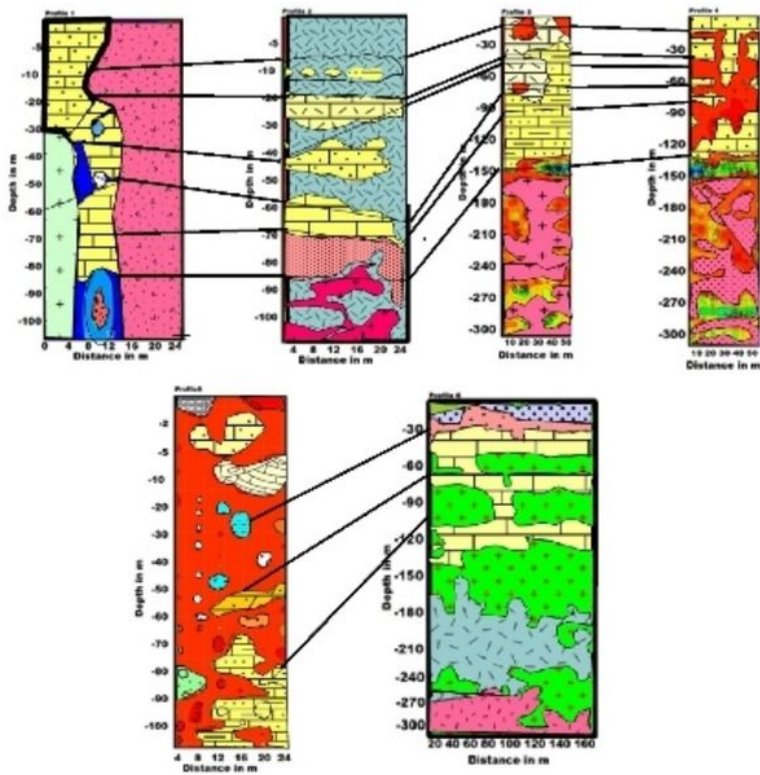


Figure 8

Magnetotelluric data compared with existing bore well where water samples collected.